THE ASTROPHYSICAL JOURNAL, 381:418–425, 1991 November 10

3C 390.3: MODELING VARIABLE PROFILE HUMPS

WEI ZHENG
Department of Physics and Astronomy, University of Alabama, Tuscaloosa, AL 35487-0324

SYLVAIN VEILLEUX
Institute for Astronomy, University of Hawaii, 2680 Woodlawn Drive, Honolulu, HI 96822

AND

STEVEN A. GRANDI
National Optical Astronomy Observatories, Tucson, AZ 85726-6732
Received 1991 March 18; accepted 1991 May 14

ABSTRACT

A comparison of the Hα and Hβ profiles of the radio galaxy 3C 390.3 at different epochs shows that the Hβ/Hα ratio is significantly higher in the line "humps" than in the rest of the profiles. No humps are found in the Lyα profile, although Lyα is as broad as the Balmer lines. Therefore, the profile humps are probably produced in a region of higher density.

A double-stream model fitted to the Hα profiles requires that the conical structure is close to the line of sight and subtends a large angle ($\geq 60°$) and a limited radial distance ($R_{max}/R_{min} \leq 10$). The pair of humps in the profile may arise from gas lumps or a narrow stream inside the cone. Fluctuations in the blue-to-red hump flux ratio may be due to variations in the relative intensity of the ionizing continuum in the two cones or to changes in the orientation of these cones. Another model is a disk with a corotating enhanced emission region ("hot patch"). With a significant angular size ($\sim 90°$), such a region would contribute a time-dependent emission component which migrates between the two humps and changes their relative intensity.

Subject headings: galaxies: individual (3C 390.3) — galaxies: internal motions — galaxies: nuclei — line profiles — radio sources: galaxies

1. INTRODUCTION

The energetic output from active galactic nuclei (AGNs) is believed to be the result of accretion onto supermassive black holes (see review by Begelman 1985). It is always an intriguing idea to seek the emission originating directly from this accretion disk. It has been suggested (Shields 1978; Malkan & Sargent 1982) that the thermal emission from accretion disks produces the UV bump observed in the spectra of many AGNs and can be used to derive the accretion rate (Sun & Malkan 1989). It has also been argued (Dumont & Collin-Souffrin 1990, and references therein) that the outer region of an accretion disk may emit low-ionization lines such as the optical Fe II and Balmer lines under the illumination of a diffuse X-ray continuum. Indeed, a small number of AGNs do exhibit very broad emission-line profiles with double humps, a feature thought to be associated with the geometry of a ring or disk. Oke (1987) and Pérez et al. (1988) argued that the double-hump profiles in the radio galaxy 3C 390.3 arise from such a disk. Chen, Halpern, & Filippenko (1989) suggested that the spectacular double-hump profiles of the Balmer lines in Arp 102B also are the signature of an accretion disk.

Many other observations, however, do not appear to support this hypothesis. One of the main problems concerns the statistics of this phenomenon: few objects show very broad lines and double-hump profiles although accretion is believed to be common in AGNs. It has been suggested that most QSOs do not exhibit significant rotational motion (Mathews 1982), as judged from the lack of flat and broad emission-line profiles. A recent analysis of Hβ profiles in many AGNs (Sulentic et al. 1990) reveals that none of them, including 3C 390.3 and Arp 102B, fits a simple thin disk model because of the lack of a large redshift in the far wings. Another challenge to the disk model arises from the fact that objects known to have double-hump profiles exhibit considerable spectral variations (Oke 1987; Miller & Peterson 1990; Veilleux & Zheng 1991). These observational results cannot be fitted with a simple disk model in which the blue hump is expected to be stronger than the red hump due to relativistic effects.

Numerous aspects of 3C 390.3 have been studied extensively: (1) its optical line intensity and profile shapes (Osterbrock, Koski, & Phillips 1975, 1976), (2) continuum and line variability (Barr et al. 1980; Yee & Oke 1981; Netzer 1982; Clavel & Wamsteker 1987), (3) narrow line ratios (Ferland et al. 1979, Netzer 1982; Veilleux 1988; Zheng & Pérez 1991), and (4) the substructure of the broad Balmer lines (Oke 1987; Pérez et al. 1988). Veilleux & Zheng (1991, hereafter Paper I) recently presented a comprehensive report of the broad Hβ profile over 14 yr. Their main findings include the following. (1) The ratio of blue-to-red hump strengths of the Hβ profile has varied in a regular, nearly sinusoidal pattern with a time interval between the maxima of 10.4 yr. (2) The blue hump has shown a slow velocity shift of about $+900$ km s^{-1} over the 14 yr interval of the observations. (3) A third, highly redshifted hump was observed in the Balmer profiles during 1974–1975. Possible models, including light echo, binary broad line region (BLR), double-stream BLR, and inhomogeneous disk, were discussed briefly. In this paper, we present an additional analysis of the Lyα and Hα profiles (§ 2) and provide detailed fits of the two more likely models (§ 3). The results are summarized in § 4.

2. RESULTS

As a complement to Paper I, we used the Hα profile for model fits. This is because (1) the Hα profile has a better signal-to-noise ratio (S/N) than Hβ and (2) the red wing, which was

less certain in the previous study because of the [O III] contamination in the Hβ profile, can be determined with better accuracy. The main disadvantage in choosing Hα over Hβ is the presence of the atmospheric B band and the narrow Hα and [N II] lines which make the core profile within ±1500 km s^{-1} highly uncertain. Since the models depend on the wings more than on the core, fit to the Hα profile is preferred. The optical spectroscopic data were obtained, respectively, on 1976 June 30 and 1980 June 19 with the image dissector scanner on the Lick 3 m Shane telescope. A grating of 600 lines per mm was used, yielding a resolution of about 10 Å. The aperture size was 2".7 × 4". We used these two spectra to represent the two states in which the Hα profiles are strikingly different (Figs. 1*a* and 1*b*).

Differences in the wing profiles are observed between the two states, especially in the blue wing. We studied the blue and red sides of the Hα profile separately. First, the peak flux of each of the humps of the broad component was determined. Then the velocity positions where the intensity reaches three-fourths and one-fourth of this peak level were measured. The difference in velocity between these two positions was used to compare the shape of the line wings. For the blue wing, the velocity difference was approximately 2000 km s^{-1} in 1976 and 3700 km s^{-1} in 1980. The blue wing was indeed steeper in 1976 when the blue hump was stronger. The difference for the red wing was approximately 3700 km s^{-1} in 1976 and 2500 km s^{-1} in 1980. To explain these results, the hump profile must be steeper than the underlying Hα profile. It is interesting to note that both humps have similar profiles and intensities.

The *IUE* spectra of 3C 390.3 from 1978 to 1989 were retrieved from the NASA National Space Science Data Center (NSSDC). The S/N of the individual *IUE* spectra may not be high enough to reveal the corresponding humps, so we produced averaged Lyα profiles for every year. A bin size of 0.5 Å was used in the merging process to avoid additional loss of resolution. The resultant averaged Lyα profiles were smoothed by a filter of 250 km s^{-1} (1 Å). Although we were not able to find near-simultaneous UV spectra to match the optical results, it was shown in Paper I that the two humps in the optical profiles probably switched their relative intensity during the second half of 1979. The averaged spectrum of SWP 3410 and SWP 3478, acquired in 1978 November (Fig. 1*c*), therefore represents an approximate match to the Hα profile in 1976, and an averaged spectrum of SWP 9131, SWP 10753, and SWP 10907, acquired between 1980 May and December (Fig. 1*d*), corresponds to the Hα profile in 1980. Because of the broad SWP instrumental profile, the narrow Lyα component appears broader than the Hα core. However, there is no significant difference in the *broad* Lyα profile despite the striking profile difference in the corresponding Balmer lines. The averaged Lyα profiles in 1979 and 1982 were also studied, and no hump was noticed. We conclude that the hump emission must originate mainly from a region in which the Lyα/Hα ratio is low.

Although the measurements of the two humps in Hβ have been presented in Paper I, the definition of the humps in that paper was based on their visual appearance and hence was somewhat arbitrary. The dramatic profile variation between 1976 and 1980 provides an opportunity to separate the humps with improved accuracy. We normalized the spectra of 1980 to that of 1976 by the [O III] intensity and then subtracted one from the other to produce a difference spectrum. The difference spectrum shows a blue hump between −6000 and −1000 km s^{-1} and a red hump (with an opposite flux level) between +1500 and +5000 km s^{-1}. The wavelength range on the red side is smaller than on the blue side, due to the [O III] contamination of Hβ.

We then estimated the Balmer decrement of the humps using the velocity intervals determined above. The Hβ/Hα ratios of the blue and red humps are found to be 0.26 and 0.21, respectively. The Hβ/Hα ratio of the emission underlying these humps is only 0.12 for both the blue and red parts (as measured in the 1976 data). The uncertainty on these ratios is estimated to be about 20%. The narrow lines in 3C 390.3 are found to vary steadily (Zheng & Pérez 1991) so the adopted normalization may not be fully justified. We also made a direct sub-

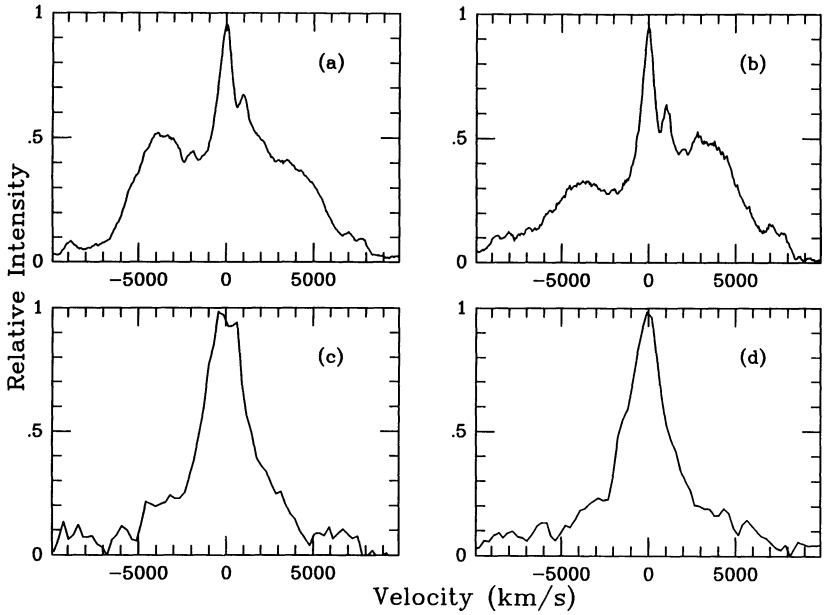

FIG. 1.—Hα profile in (*a*) 1976 and (*b*) 1980, and composite Lyα profile in (*c*) 1978 and (*d*) 1980

traction between the unscaled 1976 and 1980 spectra and found that the Hβ/Hα ratio is 0.22 and 0.28 for the blue and redhumps, respectively. Therefore, the conclusion about the higher Hβ/Hα ratio in the humps is independent of the normalization procedure used. Such a significantly higher Hβ/Hα ratio in the humps implies that they are produced in a region with considerably different physical conditions. As Kwan (1984) indicated, a higher Hβ/Hα ratio may imply a significantly higher density. The claim of Pérez et al. (1988) that the humps were visible in the (noisy) profiles of C III] needs to be reexamined carefully in view of these new results.

3. MODELS

Four possible models were briefly discussed in Paper I to explain the peculiar profile changes. Among them the light echo model appears unlikely based on time-scale arguments, while the binary BLR model, in which each component has an independent BLR, actually requires a highly unstable system consisting of *three* components to explain the two main humps and the highly redshifted feature observed in 1974–1975. We will therefore focus our attention on model fits involving a double-stream BLR or a disk with a "hot patch."

Using a conventional photoionization model one can estimate the BLR size of 3C 390.3. The continuum flux at 1300 Å is 5×10^{-15} ergs cm^{-2} s^{-1} Å^{-1}. If the continuum power index is -1, the number flux of the total ionizing photons between 13 and 100 eV is about 0.5 cm^{-2} s^{-1}, roughly one order of magnitude higher than the Lyα and Hα photon fluxes. Therefore, we estimate the covering factor of the Hα–emitting region to be 0.1. As a first-order approximation, we assume that the BLR is parts of a spherical shell of radius R_0 and thickness D_c/n, where D_c is the column density of a typical broad-line cloud and n is its density. Defining $F_{\rm H\alpha}$ as the flux of Hα, the radius of the BLR is then

$$R_0 = \left(\frac{F_{\rm H\alpha} c^2 z^2}{0.1 h\nu_{\rm H\alpha} \alpha n D_c H_0^2}\right)^{1/2} \approx \left(\frac{1.1 \times 10^{44}}{n}\right)^{1/2} \text{ cm} ,$$

using $H_0 = 50$ km s^{-1} Mpc^{-1}, $D_c = 10^{23}$ cm^{-2}, and a total Hα recombination coefficient $\alpha = 4.4 \times 10^{-14}$ cm^3 s^{-1} (for $T = 20{,}000$ K). If the density is assumed to be $n = 10^{11}$ cm^{-3}, the BLR size is roughly 0.4 lt-month. Another size estimate can be derived from the behavior of the blue-to-red flux ratio if we make the assumption that the 10.4 yr interval between the two maxima reflects the rotational period of a line-emitting disk (see § 3.2). If this is the case then the disk size would be (0.30/sin i) lt-month, where i is the inclination angle. The BLR sizes derived from these two independent methods are in agreement with one another and with the time scale derived from the emission-line variability (Oke 1987; Clavel & Wamsteker 1987). Therefore, we will use the characteristic dimension $R_0 = 0.5$ lt-month for the models discussed below.

3.1. *Double-Stream Model*

Displaced double humps may be the result of a bipolar BLR. Zheng, Binette, & Sulentic (1990) suggested that a biconical stream can produce a flat profile under certain circumstances. It would be quite natural to link displaced, variable humps with a pair of ejecta (Oke 1987).

Our goal was to fit the profile using the least number of free parameters. We therefore tried at first to fit the data with a simple bipolar BLR made of two line-emitting cones and no central component. A radial outflow configuration, $V(r) \propto r^m$, where $m > 0$, and a volume Hα emissivity, $\epsilon \propto r^p$, were assumed. It was found that this last power index does not affect the profile shape appreciably. A more important factor is the ratio of outer-to-inner radius which determines the general slope of the profile wings: a large ratio produces more peaky profiles. Note that, if the radial range of the BLR is large, the inner region would contribute appreciably to the low-velocity part of the emission and make the resulting profile a typical logarithmic one. Such a profile would also be produced if the axis of the conical structure is nearly perpendicular to the line of sight, even for a geometrically thin BLR.

The angular distribution was assumed to be a Gaussian, i.e.,

$$\epsilon = \epsilon_0 e^{-\ln 2[(\theta-\theta_0)/\theta_w]^2} .$$

The cone's orientation angle with respect to the line of sight, θ_0, does not have a strong effect on the overall profile unless the cone is nearly along the line of sight. On the other hand, the opening angle, θ_w, greatly affects the profile shape: too small an angle produces a pair of detached broad profiles, which are not present in the data. Unfortunately, a wide bipolar BLR can produce only a flat profile without prominent hump, and an additional term is therefore needed to produce the humps. Such a region could be a lump of gas, or a region of limited size so that the velocity dispersion is smaller than the wide bipolar BLR. Note that in either case it is easy to explain the results of § 2 which suggest that the gas producing these humps is of higher density than the rest of the broad-line gas. The simple model adopted in our calculations is a narrow stream along the cone's axis which contributes 20% of the total Hα emission. Thus, the bipolar stream is assumed to consist of a broad and a narrow component. An internal random velocity $V_T = 1000$ km s^{-1} is assumed in both components to obtain the desired fit.

The following parameters represent a good fit to all of the data: $\theta_0 = 40°$; θ_w(broad) $= 60°$; θ_w(narrow) $= 25°$; $V = 7000\ (R/R_0)^{0.5}$ km s^{-1}; $\epsilon(r) \propto r^{-2}$; narrow/broad component intensity = 0.2.

The additional parameters for the 1976 Hα profile are as follows.

For the red component: $R_{\rm max} = 2R_0$, $R_{\rm min} = 0.3R_0$ with a normalized intensity of 0.8.

For the blue component: $R_{\rm max} = 2R_0$, $R_{\rm min} = 0.3R_0$ with a normalized intensity of 1.0.

For the 1980 Hα profile, the red component: $R_{\rm max} = 3R_0$, $R_{\rm min} = 0.3R_0$ with a normalized intensity of 2.0; the blue component: $R_{\rm max} = 2.5R_0$, $R_{\rm min} = 0.3R_0$ with a normalized intensity of 1.0.

Different jet intensity ratios in 1976 and 1980 were assumed to account for the different hump intensities at these two epochs. The other parameters, especially the ratio between the narrow and broad components in each stream, were kept unchanged. The overall fit is plotted in Figure 2.

During 1974–1975, a third, weaker hump in the profile of broad Hβ was apparent at $v = +4600$ km s^{-1} (Paper I). This transient feature can easily be explained in the double-stream model as being the result of a small density inhomogeneity in the mass flow of the BLR which dissipated over a period of 1 year or so.

In a bipolar model, fluctuations in the blue-to-red hump ratio may be due to variations in the relative intensity of the ionizing radiation in the two cones. Further observations will

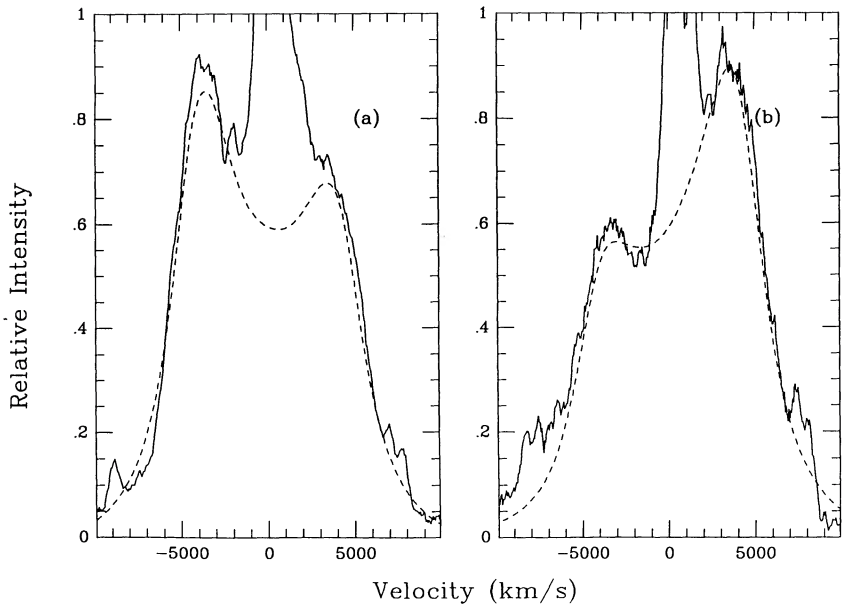

FIG. 2.—Double-stream model fit to the Hα profile in (*a*) 1976, and (*b*) 1980

determine whether or not these variations are periodic. If detected, periodicity could be explained in this model in two ways. One possibility is that the ionizing continuum is emitted in the form of a rotating searchlight. The anisotropic ionizing emission illuminates different parts of the surrounding gas, resulting in the observed changes in the hump intensity. The main difficulty with this picture is how explain the existence of such a rotating source of ionization. Another, more conservative model is that the source of ionization is not rotating but only precessing over a period of 10 yr. This would make 3C 390.3 a large-scale analog of SS 433 (Margon 1984). This concept of precession in the core of radio galaxies is not new, having been suggested to explain the peculiar morphology of radio jets in some galaxies (Ekers et al. 1978; Willis et al. 1981). The precession of the ionizing source may be due to a misalignment of the rotation axes of the acretion disk and its massive black hole, resulting perhaps from a galactic merger event. A potential problem with this hypothesis is that the time scale predicted for the precession is generally much longer than 10 yr (Rees 1978). The issue of mergers will be discussed in § 3.3.

3.2. *Disk with a Hot Region*

Profiles with a pair of variable humps have been known in the spectra of cataclysmic variables. To account for the observed periodic changes in the hump intensity of these objects, Smak (1976) proposed that variations of the line intensity and profile are attributable to the so-called D-wave and S-wave components. According to this hypothesis, the emission from an accretion disk makes the D-wave component a typical double-hump profile. In addition, there is a hot spot on the disk which corotates with the disk and produces a moving S-wave component in the emission-line profile. The S-wave component swings between the two humps and changes their relative intensity ratio (Stover 1981; Stover, Robinson, & Nather 1981).

In 3C 390.3, we found the concept of the D-wave and S-wave components useful. The change in the blue-to-red peak ratio may indeed be the result of hump migration produced by an inhomogeneous rotating disk. In a nearly edge-on position, a homogeneous ring produces an M-shaped profile with a rather sharp boundary (Gerbal & Pelat 1981). If the emitting region subtends a significant radial distance, the integrated profile would exhibit a considerable wing slope (Huang 1972). If there is an enhanced region in the disk, it produces a peak in the profile which migrates as the region corotates with the disk and changes its projection velocity.

To model the D-wave component, we applied the same basic assumptions about the disk as those used in previous models (e.g., Chen et al. 1989). As a first-order approximation, we assume a purely edge-on orientation. In 3C 390.3, the derived rotational velocity of ~ 5000 km s^{-1} is insufficient to enable distinguishing the second-order effect of the transverse Doppler term and subsequently the inclination angle. In other words, the derived velocity should actually be $V/\sin i$. Defining $\epsilon(r)$ as the Hα volume emissivity and assuming that the thin disk has a small angular extent, the line flux produced by the axisymmetrical part of the disk can be expressed as

$$L_D \propto \int \epsilon(r)\, r^2\, dr\, d\theta\ .$$

The shell emissivity is assumed to first increase with radius and then decrease beyond R_0, to make a smooth connection for a BLR with a limited radial extent. This requires that $\epsilon \propto r^m$, with $m > -3$ where $r \leq R_0$ and $m < -3$ when $r > R_0$. By choosing different values of m one can change the overall profile shape. The wings of the profiles are produced in the region between R_{min} and R_0. Strong emission from the inner region therefore yields strong wings. In contrast, the line emission between the humps is produced mainly from the region between R_0 and R_{max}. The calculations were carried out numerically by choosing $R_{min} = 0.1R_0$ and $R_{max} = 5R_0$, since the contributions from other regions are small. The radial distance was logarithmically divided into 100 sections. Because of the large radial extent of the BLR, the resultant line profile shows a pair of weak humps of equal intensity and a considerable wing slope.

Additional assumptions were introduced to model the effect of the S-wave component arising from the enhanced region.

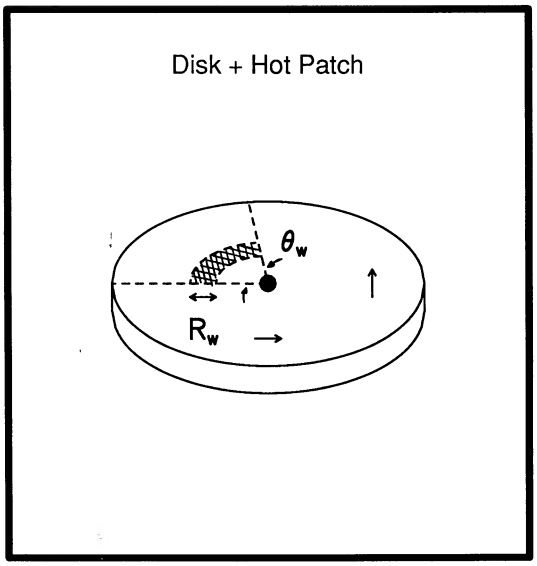

FIG. 3.—Sketch of the disk and hot patch model. R_w and θ_w, respectively, represent the radial and angular widths, where the emissivity of the hot patch drops to one-half of the peak value.

The emissivity distribution of the enhanced region was assumed to extend along both the radial and angular directions, i.e.,

$$L_S \propto \int \frac{\theta_w^2}{\theta^2 + \theta_w^2}\, d\theta \int e^{-\ln 2[(r-R_0)/R_w]^2}\, dr\ ,$$

where R_w and θ_w, respectively, represent the radial and angular widths where the emissivity drops to one-half of the peak value. A sketch of this model is presented in Figure 3.

As demonstrated in the studies of cataclysmic variables, a "hot spot" produces a sharp S-wave component which moves between the double humps. However, we found that the emission feature produced by an enhanced region which subtends a wide angle is not highly time-dependent. The S-wave component in this case is a hump with considerable line width which remains fixed for quite a long period of time before moving quickly to the other profile end. During the transition period, the hump appears very broad and is not easily distinguishable from the underlying disk emission. We found that a Lorentzian angular distribution produces a better fit to the profile wing opposite the hump. This represents a situation in which the enhanced region not only makes a significant peak, but also forms a ring of low emissivity.

Figure 4 plots the simulated peak migration and the time dependence of the blue-to-red flux ratio during a quarter of the orbital period, for enhanced regions with different angular extents. The important result to emphasize once more is that the emission feature stays near the profile edges for a significant amount of time if the region's angular extent is large. This is because the assumed width angular distribution of the enhanced region ($\sim 90°$) makes it more or less like a ring. In such a case, the region where the vector of the rotational velocity points within $\sim \pm 30°$ of the line of sight contributes significantly to the profile's far wings and makes a pair of humps not much broader than 700 km s^{-1}. This is similar to the formation of a double-hump profile in a homogeneous disk as a result of geometric projection and nonlinearity of the sinusoidal function. When the S-wave component is present in the profile core, the projection effect is minimal. The hot patch then subtends such a wide angle that it is nearly undetectable.

We found a good fit using the following parameters:

Emissivity power index: $m = -2.5$ when $r \leq R_0$;
$m = -4.6$ when $r > R_0$.

Characteristic radius: $R_0 = 5700 R_S$.

Half-width of S-wave: $\theta_w = 90°$,
$R_w = 0.1 R_0$,

where R_S is the Schwarzchild radius, estimated as 7×10^{12} cm.

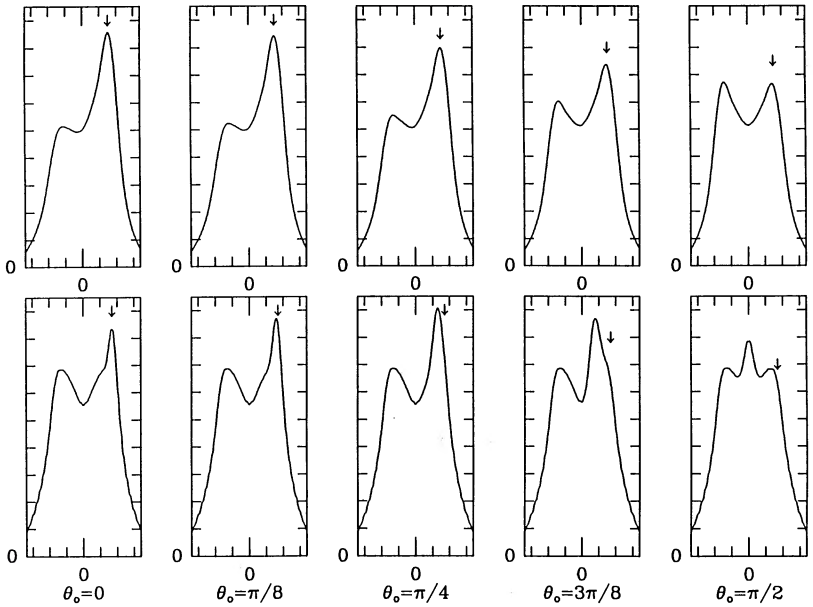

FIG. 4.—Simulated time development of the broad line profile during one-fourth of the rotational period of a disk with a hot patch with angular width θ_w. *Upper panel*, $\theta_w = 90°$; *lower panel*, $\theta_w = 10°$. Arrow marks the maximum peak shift.

The center of the S-wave component was assumed to be at P.A. = 160° in 1976 and P.A. = 20° in 1980 (where P.A. = 0° corresponds to the line of sight). This is because Figure 2 of Paper I suggests that the hump ratio reached its maximum in 1975 and minimum in 1982, and the adopted values represent the corresponding interpolated position. In 1976, the flux of the S-wave component was 21% of the D-wave component, and 25% in 1980. This assumption is needed because the Hα profiles during these years had slightly different hump intensities.

Like all other disk models, the resultant profiles have sharp boundaries and need additional local random velocity to produce a smooth fit. Chen & Halpern (1989), in their improved fit to the Hα profile of Arp 102B, suggested a random velocity as large as 2000 km s^{-1} for this object. We found that a random velocity of 1000 km s^{-1} can sufficiently improve the fit of 3C 390.3. The random velocity could be due to electron scattering (Shields & McKee 1981) or local turbulence of nonthermal nature. The sum of the D-wave and S-wave component contributions yielded the total model fit shown in Figure 5.

In this scenario, the third, highly redshifted peak noted in Paper I may be due to an inhomogeneity in a region of the accretion disk with a large recession velocity. This inhomogeneity dissipated over a short time scale, probably because it was not fed by sustained mass accretion.

The temperature and density in the enhanced region are expected to be higher than that of the overall disk. Ultraviolet emission produced by this hot patch may affect the ionization structure of the disk and have an impact on the line ratios. In fact, the lack of time delay between the continuum and the flux in the humps reported in Paper I may imply that a significant portion of the underlying optical continuum originates in the "hot patch."

3.3. *Binary Core*

The possibility of supermassive binaries in AGNs has been suggested and applied to some objects (Begelman, Blandford, & Rees 1980; Sillanpää et al. 1988). Gaskell (1983, 1988) suggested that a binary core with each having a BLR can account for the double-peaked profile structures found in some AGNs. According to this hypothesis, the rotation about the center of mass should result in a slow migration of the peak wavelength. For Arp 102B, Halpern & Filippenko (1988) found no apparent wavelength shift for the humps over a 5 yr period, and argued that a binary BLR can thus be ruled out. The situation is not as clear in 3C 390.3.

Indeed, the blue hump is found to have shifted by about +900 km s^{-1} in 14 yr (Paper I). In the binary core model, this shift may be attributed to the orbital motion of a primary object and its BLR around the center of mass of a binary core. The velocity shift of +900 km s^{-1} in 14 yr determined in Paper I yields a very rough estimate of the orbital period, on the order of 100 yr. Note that the velocities of the two humps relative to the narrow line velocity are approximately −4000 km s^{-1} and +2500 km s^{-1}; it is therefore possible that this velocity asymmetry is due to an orbital velocity of approximately −750 km s^{-1} with respect to the systemic velocity. This would suggest that the primary object is now approaching us from the near side of the orbit. In this picture, the *whole* broad line profile—not only the blueshifted hump—has shifted toward more positive velocities and is expected to continue to do so over at least the next decade. Unfortunately, our data do not allow us to verify this statement because (1) the red wing of Hβ is severely contaminated by [O III] λλ4959, 5007 and (2) the complex intensity and profile variations of Hα prevent us from obtaining a meaningful measurement of the centroid of this emission line. Monitoring of this object over a longer time scale would be very useful in that respect.

The binary core hypothesis may help explain the behavior of the blue-to-red flux ratio in the context of the two models discussed in this paper. Indeed, any misalignment between the orbital angular momentum of the binary system and the spin angular momentum of the primary black hole (to which the BLR is attached) may result in the precession of the axis of the ionizing cones postulated in the double-stream model to

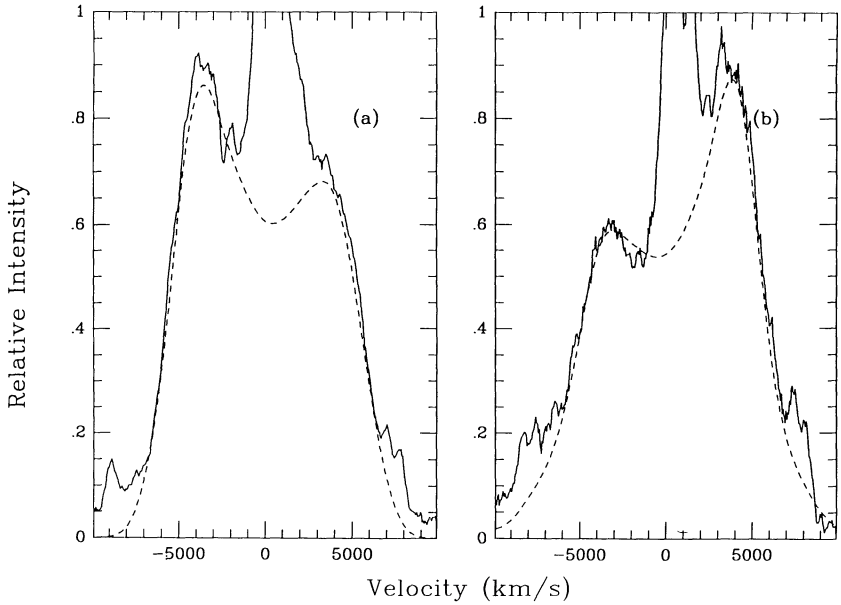

FIG. 5.—Disk model fit to the Hα profile in (*a*) 1976 and (*b*) 1980

explain the possibly periodic variations of the blue-to-red flux ratio (Bardeen & Petterson 1975). Similarly, in the inhomogeneous disk model, the presence of the second massive component in the neighborhood of the BLR induces a barlike potential which causes the surrounding material to accrete along a preferential axis, therefore producing a localized hot patch similar to what is observed in cataclysmic variables. Another possibility is that the hot patch on the disk is directly caused by the ionizing continuum emitted from the companion. Note, however, that if this last possibility applies to 3C 390.3 the companion and rotating BLR are in differential rotation, and hence the enhanced region is not rotating with the same angular speed as the BLR gas itself, as determined from the line width.

Other facts point toward a possible relationship between double-hump profiles and binary cores. 3C 390.3 is located in a rich environment of nearby galaxies (Baum et al. 1988) and is therefore a likely candidate for galaxy merger. Another object, Arp 102B, is also accompanied by a nearby galaxy, suggesting a recent encounter and the subsequent induced galactic activity. Halpern & Filippenko (1988) reported the stability of profile humps in Arp 102B over 5 yr as an argument against binary BLRs. Miller & Peterson (1990), on the other hand, found that the Hβ profile actually varied in recent years, therefore reviving the binary core hypothesis. The QSO OX 169 and Seyfert galaxy Ark 120 are two members of a group of AGNs which exhibit nearly logarithmic profiles with two slightly separated peaks. These objects may also contain a binary core but show nearly regular profiles because of different viewing angles. Stockton & Farnham (1991) recently reported that the double-peaked Hβ profile in OX 169 has changed over several years and that images of this object show a jetlike structure which may be of tidal origin. Stockton and Farnham therefore argued that the double-hump profile is associated with a binary core, possibly as the result of a merger.

4. SUMMARY

The study of the profile history of 3C 390.3 has shown the following facts that clearly support a complex model for its broad line-emitting region. (1) The relative intensity of the blue and red humps of the Balmer lines changes in a regular pattern. This rules out the standard disk model where the stronger blue hump is the result of relativistic brightening. (2) No corresponding changes in the Lyα profile were found. (3) The Hβ/Hα ratio varies with the line-of-sight velocity such that its value is higher in the humps. (4) The blueshifted hump and perhaps even the whole broad-line profile of Hα have shifted by $+900$ km s^{-1} over the 14 yr period of the observations.

The broad-line profile in 3C 390.3 can be modeled with a double-stream BLR or a disk with a corotating enhanced region. In the first model, the emission is best fitted by a biconical BLR with limited radial extent ($R_{max}/R_{min} \leq 10$) and oriented 40° from our line of sight. The BLR is made of a broad and narrow components with opening angle of 60° and 25°, respectively. Changes in the blue-to-red flux ratio may be caused by variations in the relative intensity of the ionizing continuum in the two cones or changes in the orientation of these cones. If future observations detect periodicity in this ratio, precession of the ionizing source may be the most natural explanation for this phenomenon. This precession, in turn, may be caused by the presence of a second massive component, as supported by the slow velocity shift of the blueshifted hump. In the context of the inhomogeneous disk model, a region of enhanced emission is present on the accretion disk and produces an emission hump which moves between the line wings (analog to the S-wave component of cataclysmic variables). If the region has a significant angular extent ($\sim$90°), the hump is broad when it is near the core of the lines and can be hard to detect. Such a configuration can be naturally explained in the context of a binary core in which the secondary object produces a nonaxisymmetric mass flow toward the primary component, resulting in a localized hot patch on the disk. Again, the slow shift of the blueshifted hump would be due to the orbital motion of the primary object with which the BLR is associated.

The fits used in our calculations were mainly aimed at providing a match to the basic profile features in two distinct states, and the parameters were chosen quite arbitrarily. The Balmer line profiles of 3C 390.3 are certainly more complex than these fits can produce. For example, the two humps only show similar but not exact properties.

In order to understand the details of the hump intensity and profile variations and to make a more accurate fit, a long-term monitoring project is critically needed. Basic information on the BLR configuration can be obtained from the time delay of different parts of the Balmer emission line profile. For example, in the case of bipolar outflow, the response to the continuum variations should develop from the blue wing, through the core to the red wing. In the case of an edge-on disk, both the blue red wings would respond simultaneously, and the hump may exhibit a different time delay, depending on the angular position of the enhanced region in the disk. Both wings should have a smaller time delay to the continuum variations than the core. 3C 390.3 sometimes exhibits considerable variation in weeks, providing chances to test these models. In general, if both wings vary nearly simultaneously, the disk model will be in favor, and vice versa. Simultaneous UV spectroscopic observations would also be important to determine whether the UV lines respond to the continuum variations with a similar time delay.

The *IUE* data used in the analysis were provided by NASA NSSDC. W. Z. acknowledges the support of EPSCoR grant RII-8996152, provided jointly by NSF and the state of Alabama. S. V. would like to acknowledge the financial support of the National Science Foundation under grant NSF AST 88-18900 and the Natural Sciences and Engineering Research Council of Canada through a postdoctoral fellowship. We thank D. E. Osterbrock for comments on an earlier version of this paper.

REFERENCES

Bardeen, J. M., & Petterson, J. A. 1975, ApJ, 195, L65
Barr, P., et al. 1980, MNRAS, 193, 549
Baum, S. A., Heckman, T., Bridle, A., van Breugel, W., & Miley, G. 1988, ApJS, 68, 643
Begelman, M. C. 1985, in Astrophysics of Active Galaxies and Quasi-Stellar Objects, ed. J. S. Miller (Mill Valley, CA: University Sciences), 411
Begelman, M. C., Blandford, R. D., & Rees, M. J. 1980, Nature, 287, 307
Chen, K., & Halpern, J. P. 1989, ApJ, 344, 115
Chen, K., Halpern, J. P., & Filippenko, A. V. 1989, ApJ, 339, 742
Clavel, J., & Wamsteker, W. 1987, ApJ, 320, L9
Dumont, S., & Collins-Souffrin, S. 1990, A&A, 229, 313
Ekers, R. D., Fanti, R., Lari, C., & Parma, P. 1978, Nature, 276, 588
Ferland, G. J., Rees, M. J., Longair, M. S., & Perrymann, M. A. C. 1979, MNRAS, 187, 65P

Gaskell, C. M. 1983, in Quasars and Gravitational Lenses, Proc. 24th Liège Internat. Ap. Coll. (Liège: Institut d'Astrophysique, Université de Liège), 473
———. 1988, in Active Galactic Nuclei, ed. H. R. Miller and P. J. Wiita (Berlin: Springer), 61
Gerbal, D., & Pelat, D. 1981, A&A, 95, 18
Halpern, J. P., & Chen, K. 1989, in IAU Symposium 134, Active Galactic Nuclei, ed. D. E. Osterbrock & J. S. Miller (Dordrecht: Kluwer), 245
Halpern, J. P., & Filippenko, A. V. 1988, Nature, 331, 46
Huang, S.-S. 1972, ApJ, 171, 549
Kwan, J. 1984, ApJ, 283, 70
Malkan, M. A., & Sargent, W. L. W. 1982, ApJ, 254, 22
Margon, B. 1984, ARA&A, 22, 507
Mathews, W. G. 1982, ApJ, 258, 425
Miller, J. S., & Peterson, B. M. 1990, ApJ, 361, 98
Netzer, H. 1982, MNRAS, 198, 589
Oke, J. B. 1987, in Superluminal Radio Sources, ed. J. A. Zensus & T. J. Pearson (Cambridge: Cambridge University Press), 267
Osterbrock, D. E., Koski, A. T., & Phillips, M. M. 1975, ApJ, 197, L41
———. 1976, ApJ, 206, 898
Pérez, E., Penston, M. V., Tadhunter, C., Mediavilla, E., & Moles, M. 1988, MNRAS, 230, 353
Rees, M. J. 1978, Nature, 275, 516
Shields, G. A. 1978, Nature, 272, 706
Shields, G. A., & McKee, C. F. 1981, ApJ, 246, L57
Sillanpää, A., Haarala, S., Valtonen, M. J., Sundelius, B., & Byrd, G. G. 1988, ApJ, 325, 628
Smak, J. 1976, Acta Astr., 26, 277
Stockton, A., & Farnham, T. 1991, ApJ, 371, 525
Stover, R. J. 1981, ApJ, 248, 684
Stover, R. J., Robinson, E. L., & Nather, R. E. 1981, ApJ, 248, 696
Sulentic, J. W., Calvani, M., Marziani, P., & Zheng, W. 1990, ApJ, 355, L15
Sun, W., & Malkan, M. A. 1989, ApJ, 346, 68
Veilleux, S. 1988, AJ, 95, 1695
Veilleux, S., & Zheng, W. 1991, ApJ, 377, 89 (Paper I)
Willis, A. G., Strom, R. G., Bridle, A. H., & Fomalont, E. B. 1981, A&A, 95, 250
Yee, H. K. C., & Oke, J. B. 1981, ApJ, 248, 472
Zheng, W., Binette, L., & Sulentic, J. W. 1990, ApJ, 365, 115
Zheng, W., & Pérez, E. 1991, in Variability in AGN, ed. H. Miller & P. Wiita (Cambridge: Cambridge University Press), in press